AMERICAN SOCIETY FOR MICROBIOLOGY | Infection and Immunity

Immunology | Full-Length Text

Characterization of the immunosuppressive environment induced by larval *Echinococcus granulosus* during chronic experimental infection

Leticia Grezzi,[1,2] Yamila E. Martínez,[1,2] Anabella A. Barrios,[2] Álvaro Díaz,[2] Cecilia Casaravilla[1]

AUTHOR AFFILIATIONS See affiliation list on p. 17.

ABSTRACT The larval stage of *Echinococcus granulosus* causes the chronic infection known as cystic echinococcosis, deploying strong inhibitory mechanisms on host immune responses. Using experimental intraperitoneal infection in C57BL/6 mice, we carried out an in-depth analysis of the local changes in macrophage populations associated with chronic infection. In addition, we analyzed T cells and relevant soluble mediators. Infected animals showed an increase in local cell numbers, mostly accounted for by eosinophils, T cells, and macrophages. Within macrophage populations, the largest increases in cell numbers corresponded to resident large peritoneal macrophages (LPM). Monocyte recruitment appeared to be active, as judged by the increased number of monocytes and cells in the process of differentiation towards LPM, including small (SPM) and converting peritoneal macrophages (CPM). In contrast, we found no evidence of macrophage proliferation. Infection induced the expression of M2 markers in SPM, CPM, and LPM. It also enhanced the expression of the co-inhibitor PD-L1 in LPM, SPM, and CPM and induced the co-inhibitor PD-L2 in SPM and CPM. Therefore, local macrophages acquire M2-like phenotypes with probable suppressive capacities. Regarding T cells, infection induced an increase in the percentage of $CD4^+$ cells that are $PD\text{-}1^+$, which represent a potential target of suppression by $PD\text{-}L1^+/PD\text{-}L2^+$ macrophages. In possible agreement, $CD4^+$ T cells from infected animals showed blunted proliferative responses to *in vitro* stimulation with anti-CD3. Further evidence of immune suppression in the parasite vicinity arose from the observation of an expansion in $FoxP3^+$ $CD4^+$ regulatory T cells and increases in the local concentrations of the anti-inflammatory cytokines TGF-β and IL-1Ra.

KEYWORDS *Echinococcus granulosus*, M2-like macrophage, PD-L1/PD-L2, immunosuppression

Echinococcus granulosus sensu lato is the species cluster of cestode parasites that causes cystic echinococcosis. Within this cluster, the most frequent species is *Echinococcus granulosus sensu stricto* (1, 2). The larval forms of these parasites (known as hydatids) infect internal organs (mainly liver and lungs) of intermediate hosts (domestic ungulates and humans), developing as fluid-filled vesicular structures. Once completely formed, the hydatids grow delimited by a thin cellular layer, the germinal layer, which is in turn protected by a thick acellular layer known as the laminated layer. The germinal layer undergoes endogenous asexual proliferation producing protoscoleces, which are the infective forms for the definitive hosts (mostly dogs). Protoscoleces have dual differentiation potential. In the dog's gut, they develop into adult worms, whereas within the intermediate hosts, protoscoleces freed by accidental rupture of a hydatid can undergo reverse development into new hydatids; the latter phenomenon is known as secondary infection (1).

Editor De'Broski R. Herbert, University of Pennsylvania, Philadelphia, Pennsylvania, USA

Address correspondence to Cecilia Casaravilla, ccasarav@higiene.edu.uy.

The authors declare no conflict of interest.

See the funding table on p. 17.

Received 17 July 2023
Accepted 27 November 2023
Published 4 January 2024

Knowledge on the host-parasite interaction in natural infections is mostly limited to histopathological observations (3, 4). By far, the largest body of information has been obtained from experiments using secondary intraperitoneal infection in mice, which takes advantage of the mentioned capacity of protoscoleces to generate new hydatids in an intermediate (including experimental) host. Based on these experimental studies, *E. granulosus* infections have been divided into two phases: the early or establishment phase, when the parasite is more susceptible to immune attack, and the late or established phase (also called chronic stage), during which the parasite is protected by its laminated layer and therefore more resistant to immune attack (5). Hydatids grow in their tissue niche throughout the established phase and eventually become fertile (5, 6). During early infection, the parasite induces a cellular inflammatory response that comprises neutrophils, macrophages, and eosinophils recruited during the first 3–5 days of infection; these cells persist, together with lymphocytes, until the established phase arises (7). The commencement of the established phase coincides with the deployment of immune evasion mechanisms, usually leading to the inflammatory response being mostly resolved (8). From this point on, the hydatid grows slowly in the organ parenchyma up to a size that may exceed 20 cm in diameter, chronically surrounded by a capsule of collagen fibers, which is only poorly infiltrated (1, 9, 10). How the parasite achieves this control of the inflammatory response is still poorly understood.

Information on the systemic immune response in cystic echinococcosis also arises mostly from experimental infections, in which it is well established that the effector adaptive response is Th2-biased but includes Th1 components (11, 12). The limited data available on natural infections suggest a similar profile (13, 14). In addition, regulatory components are induced and superimposed on effector responses, as evidenced by the expansion of regulatory T cells (Treg cells) and the upregulation of TGF-β and IL-10 at the infection site (as studied in the liver) and blood (4, 15–18). Therefore, similar to other helminths, in order to survive, the *E. granulosus* larva stimulates the inhibitory circuits inherent to the host's immune system, blunting the Th effector responses (19).

Information on how the established phase of *E. granulosus* infection affects the local immune environment in the experimental model is scarce. Wang et al. observed, in animals transplanted with micro-hydatids obtained by protoscolex culture, the expression of the M2 markers Chil-3, Relm-α, and arginase-1 by conventional PCR in a purified macrophage fraction (20). In agreement, Cao et al. observed the induction of arginase-1 at the mRNA and protein levels both in peritoneal macrophage and non-macrophage cell fractions, starting on the third month of infection (21). Both of these studies were carried out on BALB/c mice, which are highly susceptible to infection with *E. granulosus* (22) and the most widely used strain.

In this work, we carried out an in-depth study of the local immune environment established during the late (chronic) phase of secondary experimental cystic echinococcosis, in the relatively resistant C57BL/6 strain. We focused on the analysis of the different populations of monocytes/macrophages present at the infection site (peritoneal cavity), evaluating the expression of several M2-like phenotype markers, among other parameters. We also evaluated changes in T cell populations and relevant soluble mediators. We found that the peritoneal cavity milieu of chronically infected mice displays several signs of immunosuppressive mechanisms at play, including the induction of monocyte/macrophage populations with an M2-like anti-inflammatory phenotype, the expansion of Treg cells, and the preponderant presence of anti-inflammatory cytokines such as TGF-β and IL-1Ra.

MATERIALS AND METHODS

Parasites

Protoscoleces were obtained from naturally infected cattle from Uruguay. Infected organs (usually lungs) were collected at local abattoirs and processed in the lab. Protoscoleces were extensively washed with sterile saline solution in a laminar flow

cabinet. Viability was determined using the eosin vital stain. Only batches with more than 95% viability were used. Parasite genotype was determined according to reference (23). All the batches of protoscoleces used corresponded to *E. granulosus sensu stricto*, genotype G1.

Mouse infections

Female C57BL/6 mice were obtained from DILAVE (MGAP, Uruguay) and kept at the animal house of the Instituto de Higiene (UdelaR, Uruguay). Mice, 9–12 weeks old, were infected intraperitoneally (i.p.) with 2,500 viable protoscoleces per mouse in 200 µL of sterile saline solution. Control animals were injected with the same volume of vehicle. All the mice were kept at the animal house for 6–7 months, which corresponds to the late chronic infection phase. The procedure was approved by the Comisión Honoraria de Experimentación Animal (CHEA, Universidad de la República, Uruguay: protocol 101900-001096-19).

Peritoneal lavage

Mice were euthanized using the anesthetic isofluorane and peritoneal lavages carried out using cold RPMI medium supplemented with 0.2% (vol/vol) fetal bovine serum, penicillin, streptomycin, and amphotericin B (lavage medium). The first lavage was carried out with 1 mL of lavage medium, and this was followed by two additional lavages with 5 mL each. After lavage, the peritoneal cavity of infected mice was exposed and hydatids were collected to estimate parasite load, both in terms of numbers of hydatids and total parasite volume. The first peritoneal lavage was spun, and the supernatant was kept at −20°C for the measurement of soluble mediators. Peritoneal exudate cells (PEC) were recovered from the pooled pellets of the three lavages and kept on ice. They were counted using the Nexcelom K2 Cellometer and the acridine orange/propidium bromide viability stain (Nexcelom Bioscience, USA). PEC were used for measuring arginase activity and analysis by flow cytometry and qPCR, as described below.

Flow cytometry

Four hundred thousand cells per sample were stained with the Live/Dead Fixable Green Cell Stain Kit according to the manufacturer's instructions (Life Technologies, Thermo Fisher). Then, non-specific binding sites were blocked by incubating on ice with 1 µg/mL of anti-CD16/CD32 (Biolegend) and 10% (vol/vol) normal rat serum in FACS buffer [0.5% (wt/vol) bovine seroalbumin (BSA) and 2 mM EDTA in phosphate-buffered saline]. After blocking, the cells were surface-stained, washed twice, fixed in 1% (wt/vol) PFA (Sigma), washed again, and kept in FACS buffer. The details of the viability probe and antibodies are given in Table S1. For intracellular staining of Relm-α (from resistin-like molecule α) or Chil-3 (from chitinase-like protein 3, synonym Ym-1), after fixation, cells were permeabilized overnight with Permeabilization Buffer (eBioscience, Thermo Fisher) and then intracellularly stained as described in reference (24). For FoxP3 and Ki-67 intracellular staining, cells were fixed and permeabilized using the Foxp3 Transcription Factor Fixation/Permeabilization reagent (Invitrogen, Thermo Fisher) prior to staining with the corresponding antibodies. All the samples were acquired in a FACS Canto II Cytometer (BD Biosciences) and analyzed using the FlowJo software package. The expression level of molecules of interest was estimated in terms of ΔGeoMean. This is the difference between the geometric mean of fluorescence intensity of the cells positive for the molecule and that of the cells negative for the molecule (within the gate of interest). The boundary between positive and negative cells was established on the basis of Fluorescence Minus One (FMO) controls.

ELISA and arginase activity assays

Cytokines were detected in samples of peritoneal lavage fluid by ELISA, using commercial kits, according to the manufacturer's instructions: TNFα, IL-6, IL-10, and IL-5 using

OptEIA kits from BD Biosciences and IL-1-β, TGF-β, IL-1Ra, Chil-3, IL-13, and IL-17A using DuoSet ELISA Systems from RnD Systems. IL-12/23p40, Relm-α, and IFN-γ were measured using non-labeled and biotin-labeled paired antibodies, followed by streptavidin-peroxidase (Thermo Fisher). For IL-12/23p40 ELISA, a monoclonal antibody from clone C15.6 (BD Biosciences) was used as a capture antibody and a biotinylated monoclonal antibody from clone C17.8 (Biolegend) was used as a detection antibody. For Relm-α ELISA, non-biotinylated and biotinylated polyclonal antibodies were used as capture and detection antibodies, respectively (PeproTech). For IFN-γ ELISA, a monoclonal antibody from clone R4.6A2 (Judith E. Allen's lab, University of Manchester) was used as a capture antibody and a biotinylated monoclonal antibody from clone XMG1.2 (Biolegend) was used as a detection antibody.

Arginase activity was measured by colorimetry in terms of urea produced from the hydrolysis of exogenous L-arginine added to 0.1% (wt/vol) Triton X-100 cell extracts, as described elsewhere (25).

Preparation of cell samples enriched in monocytes/macrophages

PEC samples were washed and incubated at 4°C with a cocktail of biotinylated antibodies against CD19, TCR-β, and SiglecF to enrich the preparation in monocyte/macrophage populations by negative affinity. The amounts of the antibodies were optimized for samples obtained from control and infected mice; representative enrichment results are shown in Fig. S4. After the incubation, cells bound to antibodies were pulled out using streptavidin-conjugated magnetic beads and a magnet (Dynabeads, Thermo Fisher), according to the manufacturer's instructions. The resulting preparation contained 95% and 94% of monocytes/macrophages/dendritic cells over total cells for samples derived from control and infected mice, respectively. Within the monocyte/macrophage/dendritic cell population, 70% and 71% were LPM for samples derived from control and infected mice, respectively (the rest being monocytes/SPM and dendritic cells).

qPCR

The expression of phenotypic makers and soluble mediators was assessed by qPCR on preparations of PEC enriched in monocytes/macrophages. Briefly, RNA extraction was carried out using TRIzol (Invitrogen), and DNA contamination was eliminated by DNase I treatment (Invitrogen) following the manufacturer's recommendations. cDNA was then obtained from 1 µg of RNA per sample using MMLV-RT (Invitrogen). qPCR reactions were performed using mouse-specific primers for Relm-α, Chil-3, Arg-1, PD-L1, PD-L2, CD206, MMP-9, CD86, CD80, MHCII, IL-10, TGF-β, IL-1Ra, IL-1R2, IL-1β, TNF-α, and IL-6. The primer sequences are shown in Table S2. Following the manufacturer's instructions, the QuantiTest SYBR Green PCR Kit (Qiagen) and a Rotor-Gene Q real-time PCR cycler (Qiagen) were used for the qPCR reactions. Conditions of cycling reactions were 95°C for 15 min, 40 cycles at 95°C for 15 s, and 60°C for 1 min, followed by a melting curve rising from 72°C to 90°C. β-2-microglobulin was used as a normalizing gene, and relative mRNA amounts were calculated using the $2^{-\Delta\Delta Ct}$ method (26).

In vitro culture of PEC

In specific infection experiments, PEC from individual infected or control mice were cultured *ex vivo*. The cells were plated in U-bottom 96-well plates (Greiner) at 1.25×10^5 cells per well (in a final volume of 200 µL), in RPMI with 10% (vol/vol) fetal bovine serum supplemented with 5 µM 2-mercaptoethanol, 10 mM HEPES, penicillin, streptomycin, and amphotericin B. Then, the cells were stimulated with 1 µg/mL anti-CD3 (BD Biosciences) or vehicle only as control. After 48 h at 37°C and 5% CO_2, $CD4^+$ T cells were analyzed in terms of proliferative response by flow cytometry, using Ki67 as a proliferation marker. Separate plates seeded with 5×10^5 cells per well were cultured under the same conditions but kept for 72 h to measure cytokine production in cell supernatants by ELISA (IFN-γ, IL-5, IL-17 and IL-10).

In vitro re-stimulation of splenocytes and lymph node cells

Spleens and mesenteric lymph nodes from infected and control mice were crushed through a sieve. For spleen samples, red blood cells were lysed for 2 min using a lysing buffer (Sigma-Aldrich). After counting, 2×10^6 splenocytes or 1×10^6 lymph node cells per well were plated into flat or U-bottom 96-well culture plates (Greiner), respectively, in RPMI with 10% (vol/vol) fetal bovine serum supplemented with 5 µM 2-mercaptoethanol, 10 mM HEPES, penicillin, streptomycin, and amphotericin B. Cells were left either un-stimulated or re-stimulated with hydatid fluid and kept at 37°C and 5% CO_2 for 72 h. Cytokine production was measured by ELISA of cell supernatants (IL-5, IL-1 and IL-10). Hydatid fluid was obtained from fertile hydatids. The fluid was concentrated 10 times using Ultrafree-MC centrifugal filter devices (Millipore) and then diluted 10 times in the cell culture media to re-stimulate the cells.

Statistical analyses

Data from two to seven independent experiments were plotted and analyzed together. Statistical analyses comparing control vs infected mice were carried out by the nonparametric Mann-Whitney method (GraphPad Prism software). In assays involving more than two experimental groups, the nonparametric Kruskal-Wallis test was used. When the Kruskal-Wallis test resulted in a statistic with a *P*-value < 0.05, the test was followed by the Dunn post-test, and multiplicity-adjusted *P* values were calculated using the Bonferroni method (also using GraphPad Prism). Throughout the paper, the symbols *, **, ***, and **** represent *P*-values less than 0.05, 0.01, 0.001, and 0,0001, respectively.

RESULTS

Chronic experimental infection with *E. granulosus* increases local cellularity

Analysis of the peritoneal cavities of C57BL/6, 6–7 months post-infection (p.i.) with *E. granulosus sensu stricto* showed substantial diversity in the parasite burdens, even among different animals within each experiment. The number of hydatids in 44 infected animals from seven independent experiments ranged from 1 to 141, and the size of individual hydatids ranged from 1 to 20 mm in diameter (Fig. 1a). Infection was accompanied by increased cellularity, with infected animals having a median of 19 $\times 10^6$ PEC (range 2–59 $\times 10^6$) in comparison with a median of 7 $\times 10^6$ PEC (range 3–14 $\times 10^6$) in control animals (Fig. 1b). As shown in Fig. 1c, this increase in total cell numbers was mostly due to increases in the numbers of eosinophils, T cells, and monocyte/macrophage populations. The latter were defined according to references (27, 28) as Ly6C^{high}MHCII$^-$ (recently recruited monocytes), Ly6C$^-$F4/80^{low}MHCII$^+$ (SPM; a gate also containing dendritic cells), and Ly6C$^-$F4/80^{high}MHCII^{low} (LPM). We also obtained data for the monocyte/macrophage populations defined as Ly6C$^+$MHCII$^+$ (monocytes differentiating to SPM) and Ly6C$^-$F4/80^{med}MHCII$^+$ (SPM converting to LPM, which we called CPM). To name CPM, we took into consideration the equivalent cells in the pleural cavity , previously named CCM (converting cavity macrophages) (28). Neutrophils were also identified in some infected animals but, in contrast to the rest of the results in this work, this observation was not reproducible across different experiments. All the gating strategies for PEC are provided in Fig. S1.

Among monocytes/macrophages, LPM was the population that contributed the most to the increase in cellularity. LPM proliferation was not enhanced by infection (Fig. S2). On the other hand, monocyte recruitment appeared to be active, as judged by the increased number of these cells, but also of the cells in the subsequent process of differentiation toward LPM, including monocytes differentiating to SPM, SPM, and CPM. The increases in cell numbers did not correlate with the parasite burdens, considered either in terms of the number or size of hydatids.

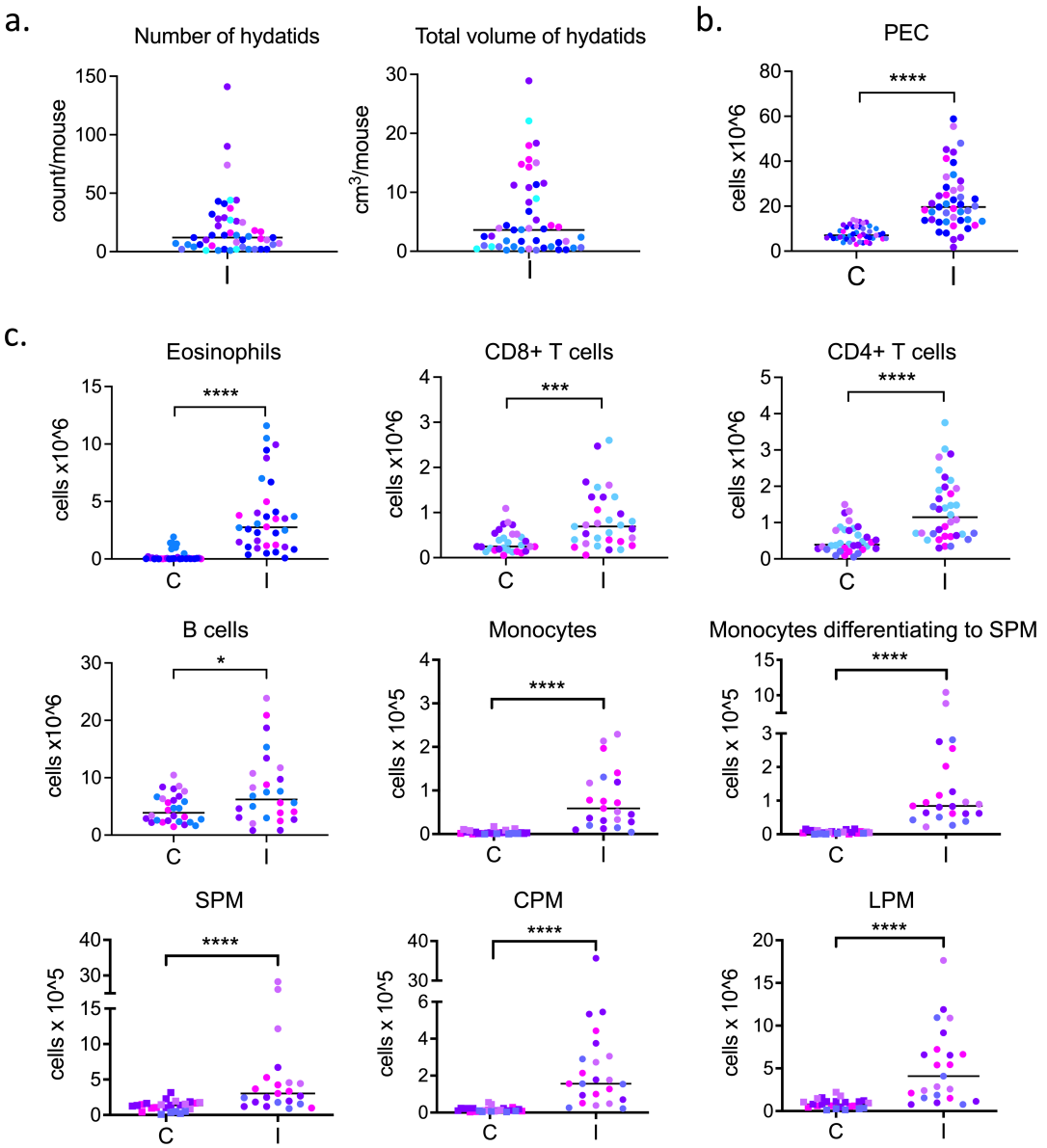

FIG 1 Chronic peritoneal infection with *E. granulosus* leads to an increase in local cellularity (PEC number). Six to seven months p.i., peritoneal lavage reveals (a) a large spread in the parasite burden recovered from infected animals, (b) a significant increase in total local cell numbers, and (c) increases in the cell numbers of all the monocyte/macrophage populations, defined as Ly6C^{high}MHCII^{-} (recently recruited monocytes), Ly6C^{+}MHCII^{+} (monocytes differentiating to SPM), Ly6C^{-}F4/80^{low}MHCII^{+} (SPM; gating including dendritic cells), Ly6C^{-}F4/80^{med}MHCII^{+} (CPM), and Ly6C^{-}F4/80^{high}MHCII^{low} (LPM). In addition, increases in SiglecF^{+} cells (eosinophils), CD19^{+} cells (B cells), and T cells (both CD4^{+} and CD8^{+}) were observed. C and I denote control and infected animals, respectively. The graphs show the results of four to seven independent experiments, analyzed together. The median value of results for each experimental group is shown. Each experiment is shown with a different color, and each dot represents one mouse.

Macrophage populations in the peritoneal cavity of infected mice exhibit M2-like phenotypes

Flow cytometry analysis of monocyte/macrophage populations revealed that SPM, CPM, and LPM exhibited M2 phenotypes (Fig. 2a), evident in terms of increases in the percentages of cells positive for the typical markers Relm-α and Chil-3 (29, 30). For monocytes and monocytes differentiating to SPM, only a slight increase in either of the two markers was observed. The increase in the expression of these markers was confirmed by qPCR analysis of a cell fraction enriched in monocytes/macrophages (Fig.

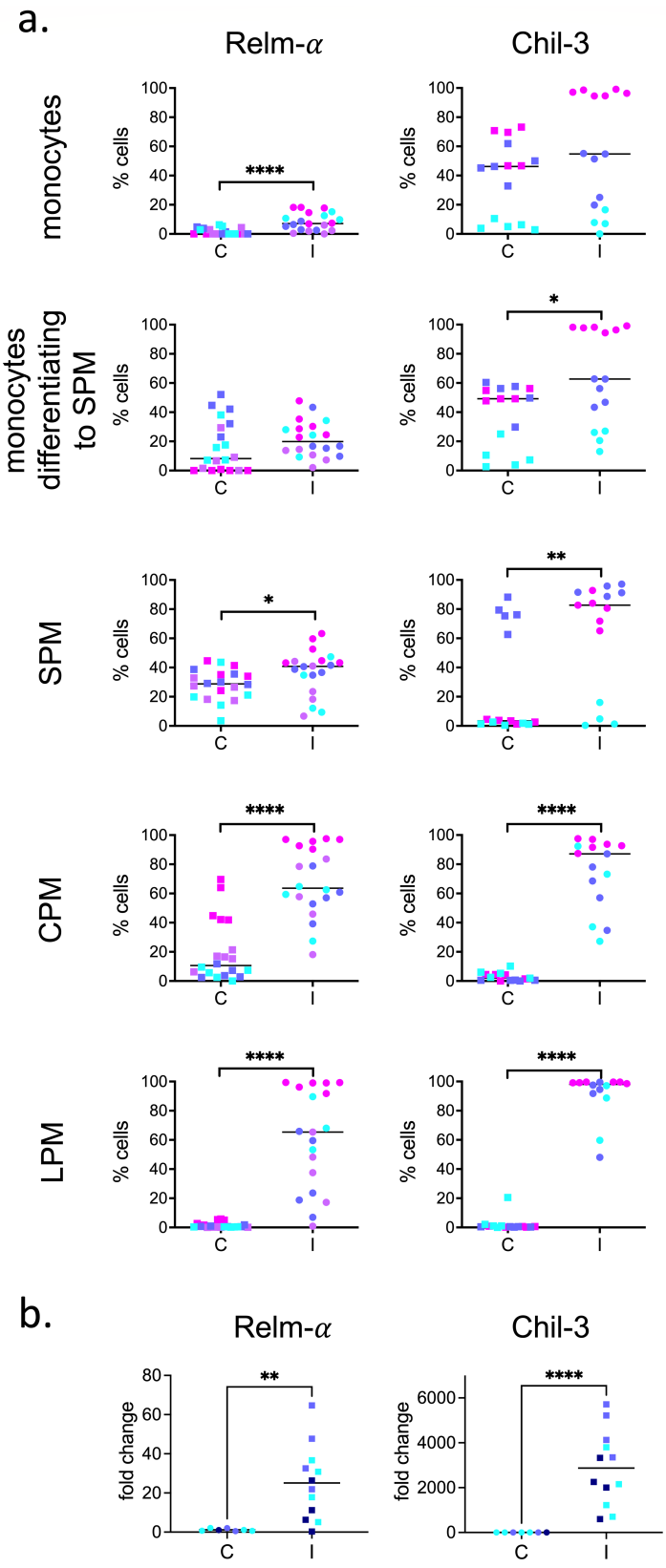

FIG 2 Local monocyte/macrophage populations during chronic experimental infection with *E. granulosus* exhibit M2-like phenotypes. Six to seven months p.i. PEC were recovered by peritoneal lavage. (a) The monocyte/macrophage populations were analyzed by flow cytometry in terms of Relm-α and Chil-3 expression. Results are shown as a percentage of Relm-α$^+$

(Continued on next page)

FIG 2 (Continued)

and Chil-3$^+$ cells within monocytes and monocytes differentiating to SPM, SPM, CPM, or LPM populations. (b) Monocytes/macrophages were purified from PEC using magnetic beads, and mRNA was isolated from the resulting fraction for qPCR analysis of Relm-α and Chil-3 expression. Fold changes in expression were calculated in relation to the median of control mice. C and I denote control and infected animals, respectively. Results are from three or four independent experiments, analyzed together. The median value of results for each experimental group is shown. Each experiment is indicated by a different color, and each dot represents one mouse.

2b; see Fig. S3 for results of a representative enrichment protocol). A milieu strongly biased toward a type 2 response was also evidenced by increase in the concentrations of Relm-α and Chil-3 in the peritoneal cavity fluid (Fig. 3).

Arginase activity, which is another of the typical markers of M2 phenotypes, also showed a very strong increase in PEC extracts from infected animals compared to control mice (Fig. 4a). When the monocyte/macrophage-enriched cell fraction was analyzed by qPCR, an increase in the expression of Arg-1 was also observed (Fig. 4b).

In one experiment, we were also able to determine that the expression of Relm-α and Chil-3 proteins and arginase activity started to be markedly elevated at 5 months p.i. and continued to rise between 5- and 7-months p.i. (Fig. S4a).

We also analyzed the expression of the co-inhibitors PD-L1 and PD-L2, of known suppressive activity (31) and expressed in M2-like macrophage phenotypes in other biological systems (32–36). By flow cytometry, we observed increases in the percentages of SPM and more markedly CPM and LPM expressing PD-L1, as well as increases in terms of median intensity of expression of the marker (ΔGeoMean, calculated as described in Materials and Methods) (Fig. 5a). A median of 98% of CPM and 96% of LPM expressed PD-L1, compared to 46% and 58% in control animals, respectively. We also observed infection-induced increases in the percentages of monocytes differentiating to SPM, CPM, and particularly SPM that expressed PD-L2. No difference in median intensity of expression of PD-L2 was observed for SPM or CPM from infected vs control animals. No expression of PD-L2 was observed in LPM from either infected or control animals. The expression of both co-inhibitors was also observed to be increased at the mRNA level (Fig. 5b). These observations suggest that monocyte-macrophage sub-types induced by *E. granulosus* infection have suppressive functions (32, 33).

Analysis of the expression of other markers previously reported to be upregulated in M2-like macrophage phenotypes revealed an increase in CD206 but no changes in CD86, CD80, MHCII, MMP-9, or IL-10 (Fig. S5).

The local presence of TGF-β and IL-1RA yields further evidence of an immunosuppressive environment

We also quantitated several pro-inflammatory and anti-inflammatory cytokines, as well as the cytokines evidencing Th lymphocyte polarization in the peritoneal fluid. IL-1β, TNF-α, IL-12/23p40, IL-5, IL-13, IL-10, IFN-γ, and IL-17A were not detected, either in infected or control mice. IL-6, TGF-β, and IL-1Ra were detected in the cavities of infected mice at significantly higher levels than in control mice (Fig. 6a). As observed for M2 markers, the concentration of TGF-β and IL-1Ra increased from 5 months p.i. onwards (Fig. S4b). We also analyzed monocyte/macrophage-enriched fractions to quantitate the expression of IL-1β, TNF-α, IL-6, TGF-β, IL-1R2, and IL-1Ra, at the mRNA level. Only IL-6, IL-1Ra, and IL-1R2 showed higher expression levels in infected mice with respect to controls, whereas the mRNA expression of IL-10 was decreased with respect to basal levels (Fig. 6b). The result for TGF-β mRNA suggests that monocytes/macrophages are not the source of the TGF-β measured at the protein level.

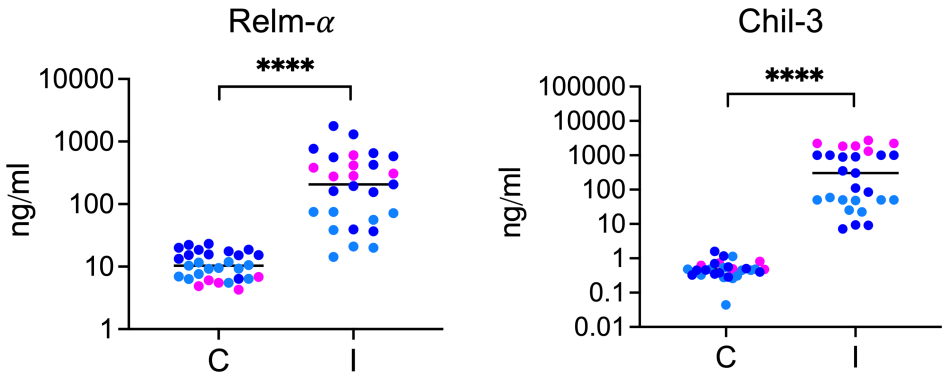

FIG 3 A type 2-biased response is also evidenced by increases in the Relm-α and Chil-3 concentrations in the peritoneal fluid. Six to seven months p.i., the peritoneal fluid was recovered by a small volume lavage (1 mL), and Relm-α and Chil-3 were quantified by ELISA. C and I denote control and infected animals, respectively. Results are from three independent experiments, analyzed together. The median value of results for each experimental group is shown. Each experiment is indicated by a different color, and each dot represents one mouse.

Chronic infection with *E. granulosus sensu stricto* is associated with the expansion of the Treg and PD-1$^+$ T cell populations

The analysis of local T cell populations present in the peritoneal cavity after 6–7 months of infection revealed that infected animals significantly expanded the Treg (FoxP3$^+$) population within CD4$^+$ cells (Fig. 7a). An increase in the percentage of PD-1$^+$ cells within the CD4$^+$ population was also observed (Fig. 7a). Bidimensional dot plot analysis of T CD4$^+$ cells showed that the FoxP3$^+$ cells were segregated from the PD-1$^+$ cells (Fig. 7b).

Local CD4$^+$ T cells from infected animals have diminished proliferative capacity

PEC from control or infected animals were cultured *in vitro* in complete medium only or in the additional presence of the polyclonal stimulus anti-CD3. CD4$^+$ T cells present in the peritoneal cavity of infected animals proliferated more than the ones in control animals in the absence of the anti-CD3 stimulus, but their capacity to respond to anti-CD3 was dampened. This suggests a hypo-proliferative phenotype in these cells, induced by the parasite (Fig. 8a). In terms of local Th polarization, the anti-CD3 stimulation experiments suggested that infection induces a mixed Th2/Th17 profile, as evidenced by trends

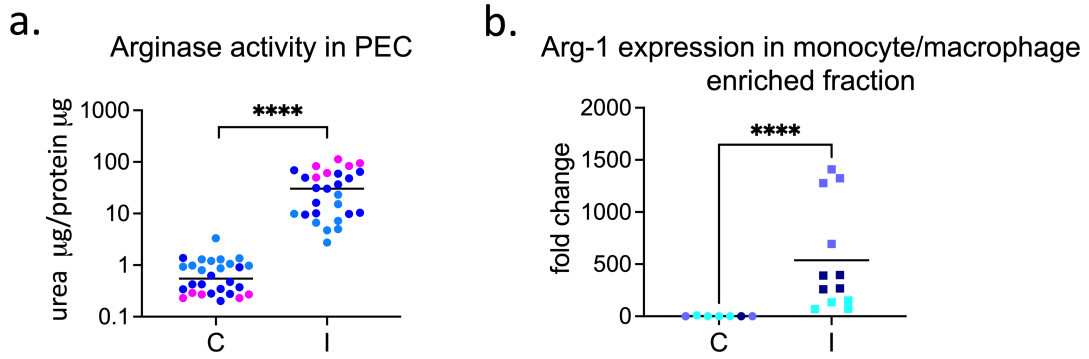

FIG 4 The type 2-biased response is confirmed by the increases in arginase activity in PEC extracts and in the expression of Arg-1 in the monocyte/macrophage populations. Six to seven months p.i., PEC were recovered by peritoneal lavage. (a) Arginase activity was measured in the total PEC in terms of the amount of urea (µg) produced by micrograms of protein present in the cell extracts. (b) Monocytes/macrophages were purified using magnetic beads, and mRNA was isolated from the resulting fraction for qPCR analysis of Arg-1 expression. Fold changes in expression were calculated in relation to the median of control mice. C and I denote control and infected animals, respectively. Results are from three independent experiments, analyzed together. The median value of results for each experimental group is shown. Each experiment is indicated by a different color, and each dot represents one mouse.

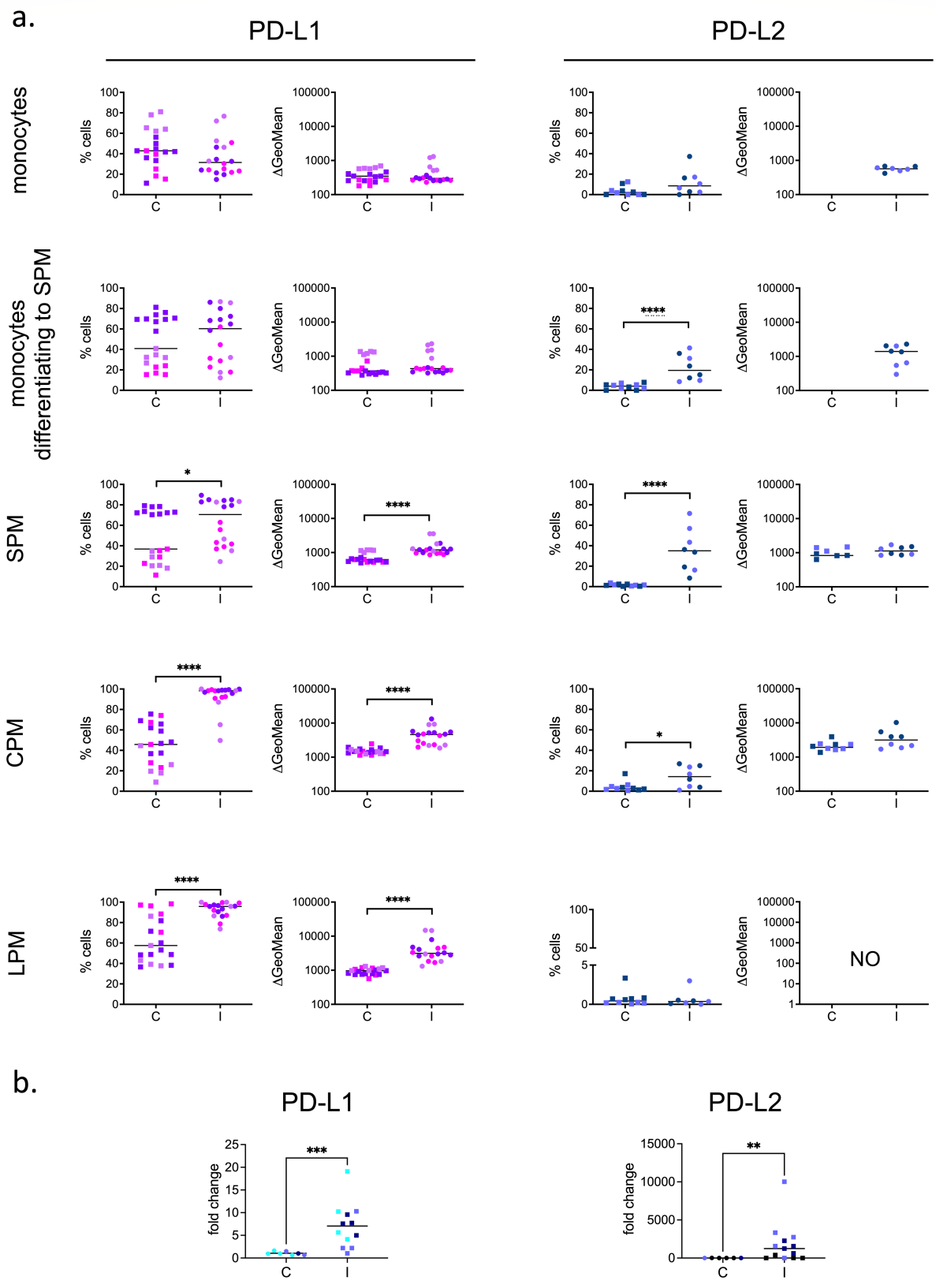

FIG 5 Local monocyte/macrophage populations during chronic experimental infection with *E. granulosus* express co-inhibitory molecules. Six to seven months p.i., PEC were recovered by peritoneal lavage. (a) The monocyte/macrophage populations were analyzed in terms of PD-L1 and PD-L2 expression by flow cytometry. Results are shown both as a percentage of PD-L1$^+$ and PD-L2$^+$ cells within monocytes and monocytes differentiating to SPM, SPM, CPM, and LPM.
(Continued on next page)

FIG 5 (Continued)

In addition, relative expression levels, estimated in terms of ΔGeoMean are shown. "NO" indicates that PD-L2 surface expression was not observed in LPM. (b) Monocytes/macrophages were purified using magnetic beads, and mRNA was isolated from the resulting fraction for qPCR analysis of PD-L1 and PD-L2 expression. Fold changes in expression were calculated in relation to the median of control mice. C and I denote control and infected animals, respectively. Results are from two or three independent experiments, analyzed together. Median value of results is indicated for each experimental group. Each experiment is indicated by a different color, and each dot represents one mouse.

toward higher IL-5 and IL-17 production and significantly lower IFN-γ production in comparison to the response of cells from control mice (Fig. 8b). In addition, cells from infected animals unexpectedly showed diminished IL-10 production in response to the polyclonal stimulus. In agreement with a local Th2/Th17-biased response, re-stimulation of cells from spleen and mesenteric lymph nodes with hydatid fluid led to significant IL-5 production and a trend toward IL-17 production in infected animals (Fig. S6). In the same assay, a trend toward IL-10 being produced by splenocytes in response to hydatid fluid was also observed.

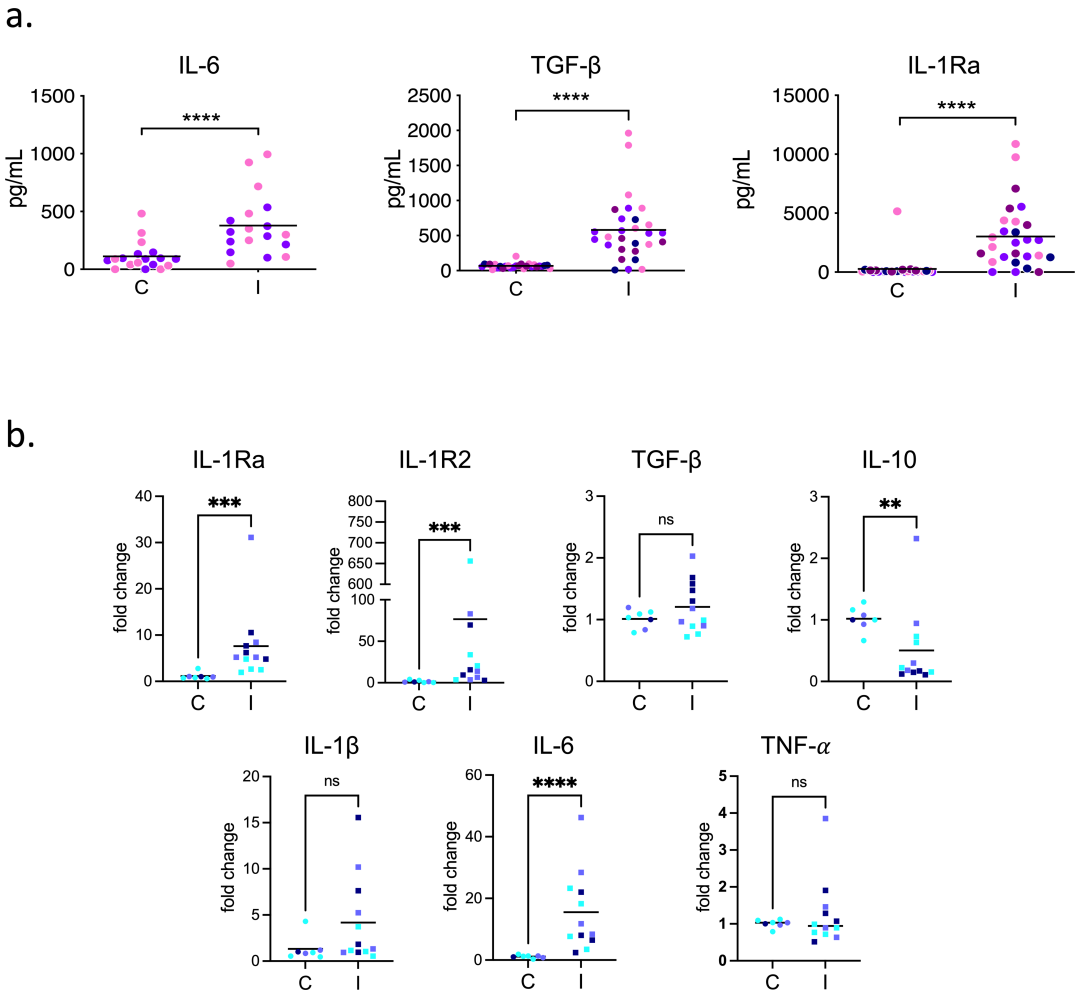

FIG 6 The peritoneal cavities of chronically infected mice are enriched in anti-inflammatory mediators. (a) IL-1β, TNF-α, IL-12/IL-23p40, IL-6, IL-5, IL-13, IFN-γ, IL-17A, IL-10, TGF-β, and IL-1Ra were measured in the peritoneal cavity fluid by ELISA. (b) mRNA coding for IL-1Ra, IL-1R2, TGF-β, IL-10, IL-1β, IL-6, and TNF-α was measured by qPCR in monocyte/macrophage-enriched fractions. Fold changes were calculated in relation to control animals. Results are from three independent experiments, analyzed together. C and I denote control and infected animals, respectively. Median value of results is indicated for each experimental group. Each experiment is indicated by a different color, and each dot represents one mouse.

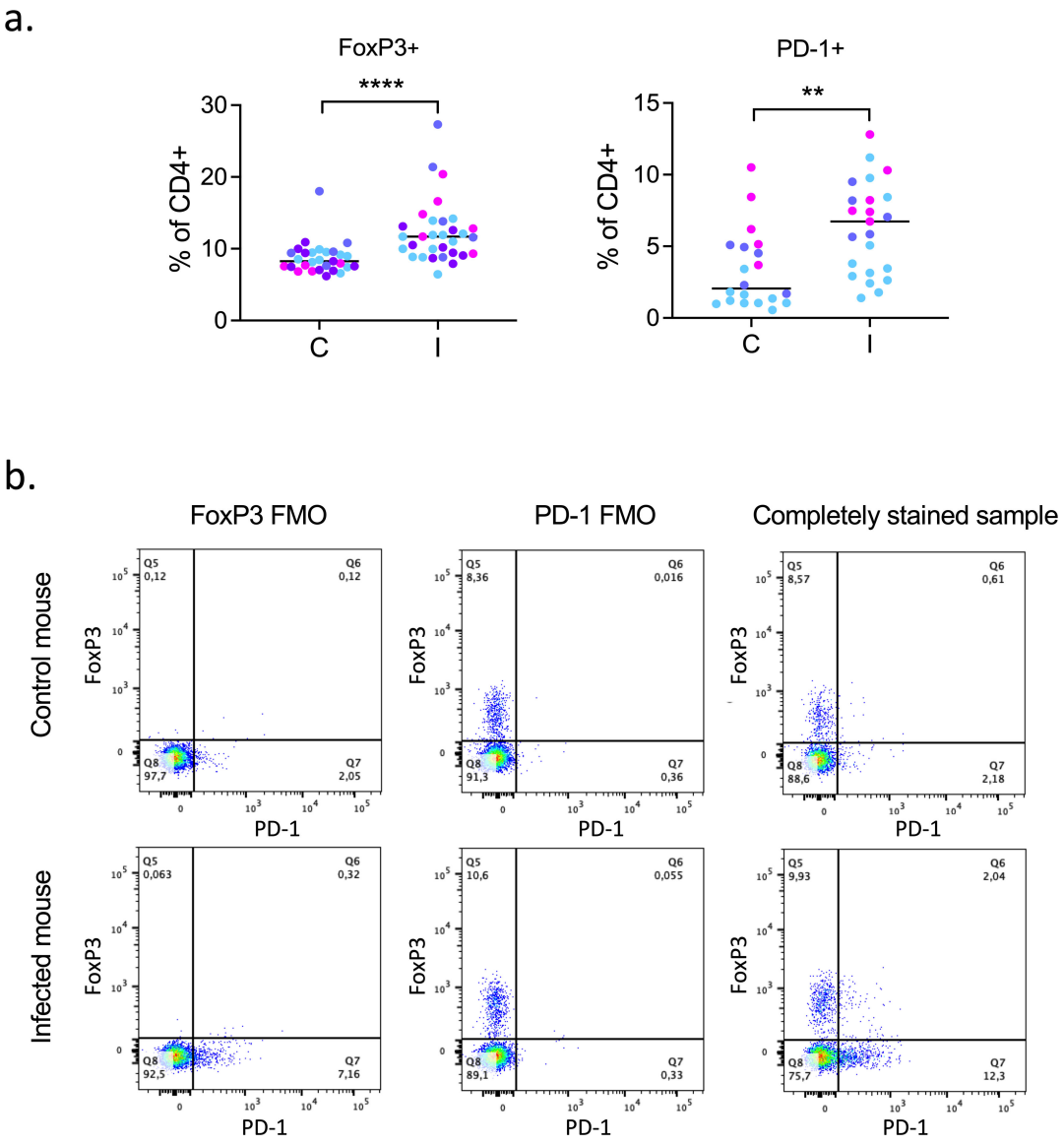

FIG 7 During chronic *E. granulosus* infection, a local expansion of FoxP3$^+$ regulatory T CD4$^+$ cells takes place, together with an increase in the PD-1$^+$ T CD4$^+$ population. T cells in the peritoneal cavity were analyzed by flow cytometry. (a) Percentages of FoxP3$^+$ and PD-1$^+$ cells among CD4$^+$ T cells are shown. C and I denote control and infected animals, respectively. Results are from three or four independent experiments, analyzed together. Median value of results is indicated for each experimental group. Each experiment is indicated by a different color, and each dot represents one mouse. (b) Representative dot plots of the FoxP3 and PD-1 FMOs and the corresponding positive samples from control or infected mice, analyzed after gating on live, CD4$^+$ T cells.

DISCUSSION

General remarks

E. granulosus hydatids develop in their intermediate hosts after overcoming an initial inflammatory response and deploying immune evasion strategies that allow their survival. Our study was focused on the local environment established once the chronic infection is established and provided clear evidence of an immune suppressive environment in terms of the phenotypes of monocyte/macrophages and T cells as well as soluble mediators. Although BALB/c mice are the most often used experimental model for *E. granulosus* infection, we chose to carry out our studies in the C57BL/6 strain, which corresponds to a less permissive immunological environment. BALB/c mice, in addition to having intrinsic defects in Th1 differentiation, generally show stronger

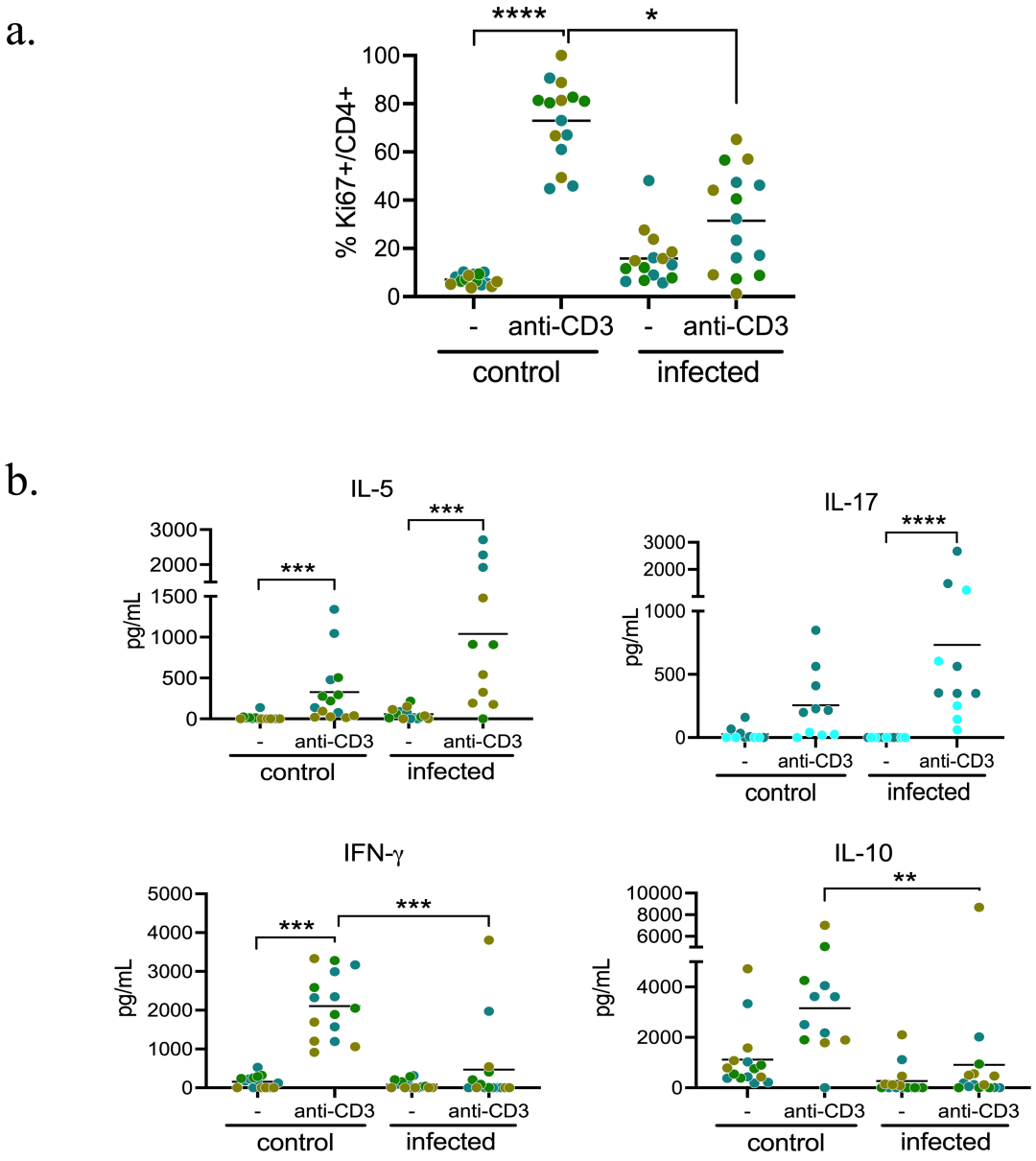

FIG 8 During chronic experimental *E. granulosus* infection, local CD4$^+$ T cells are Th2/Th17 biased, and their proliferative capacity is dampened. PEC were cultured and stimulated with anti-CD3 antibody or vehicle only as a control. (a) After 48 h incubation, cells were harvested, and the CD4$^+$ T proliferative response was evaluated by flow cytometry in terms of Ki67 expression. (b) After 72 h incubation, culture supernatants were harvested, and cytokines were measured by ELISA. Results are from two to four independent experiments. Median value of results is indicated for each experimental group. Each experiment is indicated by a different color, and each dot represents one mouse.

regulatory T cell responses (37), which probably explains their higher susceptibility to *E. granulosus* infection (22). Thus, in comparison to analogous observations that may be made in BALB/c mice, our observations in C57BL/6 mice lend a stronger level of support to the idea that this infection generates local immune suppression in its hosts.

As already pointed out by other groups (5, 6), our experiments showed that larval *E. granulosus* from a single genotype and infecting inbred hosts at the same anatomical site can show important spread in their development. In agreement with previous observations in humans (38), we did not find significant correlations between the number or size of hydatids and the intensity of any of the immune components assessed.

Chronic infection in C57BL/6 mice was accompanied by an increase in the number of PEC, as previously reported for BALB/c mice (20). This increase reflects a certain

degree of ongoing inflammation, which would be counterbalanced by the immunosuppressive environment that has also been established. Therefore, in peritoneal mouse infections, a dynamic balance between inflammation and immunosuppression appears to be installed, in place of the mostly complete inflammatory resolution observed in solid organs of suitable natural hosts (9).

Local macrophage numbers

The increase in PEC numbers observed in infected mice was mostly accounted for by eosinophils (typically recruited during helminth infections), lymphocytes, and monocyte/macrophage populations, particularly LPM. Macrophage populations in helminth infection can expand both as a result of monocyte recruitment and local proliferation (39). Our results suggest that the proliferation of monocyte/macrophage populations is not induced by experimental *E. granulosus* infection. This may relate to the capacity of particles from the parasite's laminated layer to inhibit macrophage proliferation induced either by M-CSF or by IL-4 (24). Shed laminated layer materials are effectively detected in host peritoneal cavity cells (presumably macrophages) in the BALB/c infection model (40). The increase in the numbers of monocytes and of the subsequent macrophage differentiation stages observed in our experiments suggest that the marked increase in LPM numbers observed is explained by cell recruitment from the blood. A higher potential to accomplish the differentiation pathway from monocytes to large cavity macrophages (in the pleural cavity) has been observed in C57BL/6 in comparison to BALB/c mice (28).

Local macrophage polarization

Macrophages have been described as key cells in natural *E. granulosus* infections and are also known to be present near the parasite in long-term peritoneal infections in mice (4, 6, 9). In the better-studied helminth models, including infection by the cestode *Taenia crassiceps*, macrophages are known to adopt M2-like phenotypes (30, 33). Within the umbrella of M2-like phenotypes a range of repertoires of surface and secreted molecules exists, adapted to functions such as mediating parasite expulsion, repairing damaged tissues, and resolving inflammatory responses (30, 41). Extending previous limited observations made in BALB/c mice (21, 42), we showed in C57BL/6 mice that different monocyte/macrophage populations present in the peritoneal cavity, namely SPM, CPM, and LPM, adopt M2-like phenotypes in chronic *E. granulosus* infection. In contrast to the macrophage populations mentioned, the recently arrived monocytes and the population of monocytes differentiating to SPM only showed slight increases in Relm-α or Chil-3, respectively.

Our search for additional markers previously found to be expressed in M2-like macrophages in other pathological contexts led us to conclude that TGF-β present in the peritoneal lavages of infected mice does not originate from macrophages. This stands in contrast to histopathological studies in sheep livers in which this cytokine was detected in macrophages, along with IL-10 (4).

We observed upregulation of the expression of PD-L1 and/or PD-L2 in different macrophage populations present in the peritoneal cavity of *E. granulosus*-infected mice, indicative of these cells having an immunosuppressive function. PD-L1 and/or PD-L2 expression appears to be induced in monocyte-derived cells in parallel with their differentiation into macrophages after arrival to the cavity, as no expression was detected in monocytes. The interaction of PD-L1 and PD-L2 with their receptor PD-1 on T cells is well known to dampen T cell activation and effector functions (31). A range of pathogens including helminths exploit this pathway to evade host defenses. Several studies show that these parasites induce PD-L1 and PD-L2 expression in macrophages, in cases together with M2 markers, endowing macrophages with the capacity to inhibit T effector cell populations (32–36, 43). PD-L2, in particular, is expressed in the context of helminth infections by macrophages recently derived from monocytes but not by resident macrophages (44, 45). In agreement, we observed PD-L2 expression in SPM

and to a lesser extent CPM and monocytes differentiating to SPM, but not in LPM. On the other hand, PD-L1 was constitutively expressed in macrophages and its expression was markedly increased by infection in CPM and LPM, whereas it was increased only weakly in SPM. The functional impact of the differential expression of PD-L1 and PD-L2 by local monocyte/macrophage populations in cystic echinococcosis deserves further investigation.

Local T cell response

In our PEC culture experiments, $CD4^+$ T cells from infected mice showed blunted capacity to proliferate in response to anti-CD3, suggesting a hyporesponsive state. PD-L1 and PD-L2 expressed by monocyte-macrophages may contribute, via PD-1 signaling, to this state. This hypothesis is supported by the observed increase in the percentage of PD-1^+ T cells in infected animals. Two additional factors may contribute to the hyporesponsive state of T cells in infection. One such factor is the expanded population of Treg cells, which are the most likely source of TGF-β, the local levels of which were observed to be increased by infection. The second probable factor is the very strong induction of arginase activity, which in other contexts has been reported to dampen T cell activation by inhibiting the expression of CD3ζ through L-arginine deprivation (21, 46).

PD-1 expression on the T cell surface is a consequence of cell activation. During acute infections, PD-1 is only transiently expressed. In contrast, during chronic infections, its expression is sustained, and it is a marker of a hyporesponsive or dysfunctional state in T cells known as exhaustion (31, 47). We were not able to detect the expression of additional markers of exhaustion observed in other biological models, such as CTLA-4 and LAG-3 (48). Of note, LAG-3 and the additional exhaustion marker 2B4 were shown to be expressed by liver $CD4^+$ and $CD8^+$ T cells, respectively, in mice chronically infected with *Echinococcus multilocularis* (49). It is worth noting that the function of CTLA-4 and LAG-3 is associated with inhibition of T cell activation in the lymph nodes, whereas the main function of PD-1 is to limit effector T cell activation in the periphery (31).

The ratio between the numbers of effector and Treg cells is crucial for determining effective immunity vs tolerance. In *E. granulosus* chronic infection, we determined that this ratio is diminished at the infection site, potentially contributing to the establishment of the immunosuppressed environment that favors parasite survival. These observations are in broad agreement with the expansion in Treg cells in blood all along *E. granulosus* experimental infection reported for the BALB/c mice model (50). In our experiments, we did not observe PD-1 expression in $FoxP3^+$ T cells. Therefore, although PD-L1 in the periphery is reported to be important for stable FoxP3 expression by PD-1^+-induced Treg cells (51), PD-L1/PD-L2 would not contribute to maintaining FoxP3 expression in Treg in our system.

Our study is, to our knowledge, the first to analyze the polarization of effector T cells at a cystic echinococcosis infection site. In re-stimulation assays using anti-CD3, we observed a Th2/Th17 bias. We also observed a Th2/Th17 bias after spleen and mesenteric lymph node cell re-stimulation with antigen *in vitro*. A Th2, but no Th17, bias was previously reported in chronic experimental mouse infection with *E. granulosus* but using the BALB/c experimental model (11).

Local cytokines

TGF-β, produced by Treg and/or innate cells, has been long known to play a role in helminth immunosuppression (9, 52) including infection by *E. multilocularis* (53–56). TGF-β was previously reported to be increased during chronic experimental *E. granulosus* BALB/c infections, both in terms of its serum levels and liver mRNA expression, compared to control animals (57). Our results point to an important role of TGF-β in chronic *E. granulosus* infection and also in the less regulatory C57BL/6 model.

Other groups have reported that IL-10 is an important anti-inflammatory cytokine in late experimental *E. granulosus* infections in BALB/c mice (11, 16, 58). In our experiments, we were not able to detect IL-10 in the peritoneal cavity, and in fact, infection appeared

to decrease the expression of this cytokine at the mRNA level in macrophages and the protein level in CD3-stimulated T cells. This unexpected finding, which may reflect mouse strain differences, deserves further investigation.

Our results suggest that in *E. granulosus*-infected mice, local monocytes, macrophages, and/or dendritic cells are important sources of IL-1Ra. This anti-inflammatory cytokine binds to IL-1R1, inhibiting the binding of IL-1α and IL-1β to their high-affinity receptor and thus dampening the effects of these strongly pro-inflammatory cytokines (59). Also, qPCR analysis of monocytes/macrophages from infected animals revealed an increase in the expression of IL-1R2, a decoy receptor for IL-1α and IL-1β, which acts as a sink for these cytokines without inducing pro-inflammatory effects. These observations suggest that the parasite deploys evasion mechanisms targeted to this cytokines (even if we were not able to detect IL-1β in the peritoneal cavity of infected animals). The possible deployment of evasion mechanisms against IL-1β may be related to our previous observation that particles from the *E. granulosus* laminated layer can activate the NLRP3 inflammasome in dendritic cells and macrophages primed with TLR agonists (60).

In spite of the cell recruitment observed in infected animals, we did not detect any of several important inflammatory or CD4 effector cytokines in the peritoneal cavity fluid (TNF-α, IL-1β, IL-12/23p40, IFN-γ, IL-4, IL-5, IL-13, and IL-17). It can be argued that the detection of *in vivo* changes in cytokine levels in fluids is made difficult by the uptake of the cytokines by target cells. However, the qPCR data for TNF-α in particular suggest that the infection may not cause upregulation in the expression of key inflammatory mediators (the exception being IL-6). Furthermore, certain CD4 cytokines (IL-5, IL-17) were produced by polyclonally stimulated peritoneal T cells *ex vivo*, so their lack of detection in the peritoneal fluid suggests that their production may indeed be suppressed *in vivo*.

Our failure to detect IL-4 or IL-13 at the infection site contrasts with the strong induction of M2-like macrophages observed. It is possible that factors other than IL-4/IL-13, of either parasite or host origin, may contribute to the M2-like monocyte/macrophage differentiation observed in our model (30, 61–63). Along similar lines, the lack of detection of IL-5 in the cavity fluid contrasts with the marked eosinophil recruitment to the peritoneal cavity of infected animals, as IL-5 has been described as a central regulator of eosinophilia and eosinophil activation (64).

Concluding remarks

Our work defines important immune components that contribute to the local immunosuppressive environment that allows parasite survival in cystic echinococcosis. It will be interesting to analyze the roles of the M2-like macrophage populations present in the peritoneal cavity of *E. granulosus*-infected animals, including determining if the PD-L1/PD-L2-PD-1 axis contributes to the inhibition of the T effector response. It will also be important to define the contribution of Treg cells and TGF-β to the immunosuppressive milieu induced by the parasite infection. Finally, the understanding of the parasite components involved in the induction of the observed immunosuppressive environment may lead to applications in the field of autoimmune and inflammatory disorders.

ACKNOWLEDGMENTS

The authors are indebted to Marcela Cucher (University of Buenos Aires, Buenos Aires, Argentina) for advice on *Echinococcus* genotyping.

This work was funded by CSIC I+D (Universidad de la República, Uruguay) grant number C153-348 (to C.C.) and Agencia Nacional de Investigación e Innovación (ANII; Government of Uruguay) grant FCE 156234 (to C.C.). L.G. was supported by Ph.D. scholarships from Comisión Académica de Posgrado (CAP, Universidad de la República) and ANII, and Y.E.M. and A.A.B. were supported by Master and Ph.D. scholarships from CAP, respectively.

L.G. was involved in the conceptualization, investigation, and formal analysis. Y.E.M. and A.A.B. contributed to the investigation. A.D. conceptualized and supervised the study and reviewed and edited the manuscript. C.C. was involved in conceptualization, investigation, formal analysis, funding acquisition, project administration, supervision, and original draft preparation.

AUTHOR AFFILIATIONS

[1]Laboratorio de Inmunología, Instituto de Química Biológica, Facultad de Ciencias/Instituto de Higiene, Universidad de la República, Montevideo, Uruguay
[2]Área Inmunología, Departamento de Biociencias, Facultad de Química/Instituto de Higiene, Universidad de la República, Montevideo, Uruguay

AUTHOR ORCIDs

Álvaro Díaz http://orcid.org/0000-0001-5375-6766
Cecilia Casaravilla http://orcid.org/0000-0002-2793-2161

FUNDING

Funder	Grant(s)	Author(s)
UdelaR | Comisión Sectorial de Investigación Científica (CSIC)	C153-348	Cecilia Casaravilla
Agencia Nacional de Investigación e Innovación (ANII)	FCE 156234	Cecilia Casaravilla

AUTHOR CONTRIBUTIONS

Leticia Grezzi, Formal analysis, Investigation | Yamila E. Martínez, Investigation | Anabella A. Barrios, Investigation | Álvaro Díaz, Conceptualization, Supervision, Writing – review and editing | Cecilia Casaravilla, Conceptualization, Formal analysis, Funding acquisition, Investigation, Project administration, Supervision, Visualization, Writing – original draft

ETHICS APPROVAL

Mouse studies followed the ARRIVE guidelines. Experimental protocols were individually reviewed and approved by the Institutional Animal Ethics Committees of the Universidad de la República, Uruguay, as detailed in the Materials and Methods section.

ADDITIONAL FILES

The following material is available online.

Supplemental Material

Supplemental material (IAI00276-23-S0001.pdf). Tables S1 and S2; Figures S1 to S6.

REFERENCES

1. Thompson R. 2017. Biology and systematics of *Echinococcus*, *Echinococcus* and echinococcosis, part A, p 65–109. In Thompson RCA, Deplazes PLA (ed), Advances in parasitology. Elsevier.
2. Cucher MA, Macchiaroli N, Baldi G, Camicia F, Prada L, Maldonado L, Avila HG, Fox A, Gutiérrez A, Negro P, López R, Jensen O, Rosenzvit M, Kamenetzky L. 2016. Cystic echinococcosis in South America: systematic review of species and genotypes of *Echinococcus granulosus* sensu lato in humans and natural domestic hosts. Trop Med Int Health 21:166–175. https://doi.org/10.1111/tmi.12647
3. Smyth J, Heath D. 1970. Pathogenesis of larval cestodes in mammals. Helminthol Abstr Ser A 39:1–23.
4. De Biase D, Prisco F, Pepe P, Bosco A, Piegari G, d'Aquino I, Russo V, Papparella S, Maurelli MP, Rinaldi L, Paciello O. 2023. Evaluation of the local immune response to hydatid cysts in sheep liver. Vet Sci 10:315. https://doi.org/10.3390/vetsci10050315
5. Rogan MT, Bodell AJ, Craig PS. 2015. Post-encystment/established immunity in cystic echinococcosis: is it really that simple? Parasite Immunol 37:1–9. https://doi.org/10.1111/pim.12149
6. Richards KS, Arme C, Bridges JF. 1983. *Echinococcus granulosus* equinus: an ultrastructural study of murine tissue response to hydatid cysts. Parasitology 86 (Pt 3):407–417. https://doi.org/10.1017/s0031182000050605
7. Rogan MT, Craig PS. 1997. Immunology of *Echinococcus granulosus* infections. Acta Trop 67:7–17. https://doi.org/10.1016/s0001-706x(97)00055-7
8. Breijo M, Anesetti G, Martínez L, Sim RB, Ferreira AM. 2008. *Echinococcus granulosus*: the establishment of the metacestode is associated with control of complement-mediated early inflammation. Exp Parasitol 118:188–196. https://doi.org/10.1016/j.exppara.2007.07.014

9. Díaz Á, Sagasti C, Casaravilla C. 2018. Granulomatous responses in larval taeniid infections. Parasite Immunol 40:e12523. https://doi.org/10.1111/pim.12523
10. Brehm K, Koziol U. 2017. Echinococcus-host interactions at cellular and molecular levels. Adv Parasitol 95:147–212. https://doi.org/10.1016/bs.apar.2016.09.001
11. Wang H, Li J, Pu H, Hasan B, Ma J, Jones MK, Zheng K, Zhang X, Ma H, McManus DP, Lin R, Wen H, Zhang W. 2014. *Echinococcus granulosus* infection reduces airway inflammation of mice likely through enhancing IL-10 and down-regulation of IL-5 and IL-17A. Parasit Vectors 7:522. https://doi.org/10.1186/s13071-014-0522-6
12. Díaz Á. 2017. Immunology of cystic echinococcosis (hydatid disease). Br Med Bull 124:121–133. https://doi.org/10.1093/bmb/ldx033
13. RiganÒ R, Profumo E, Di Felice O, Ortona E, Teggi A, Siracusano A. 2008. *In vitro* production of cytokines by peripheral blood mononuclear cells from hydatic patients. Clin Exp Immunol 99:433–439. https://doi.org/10.1111/j.1365-2249.1995.tb05569.x
14. Riganò R, Buttari B, De Falco E, Profumo E, Ortona E, Margutti P, Scottà C, Teggi A, Siracusano A. 2004. *Echinococcus granulosus*-specific T-cell lines derived from patients at various clinical stages of cystic echinococcosis. Parasite Immunol 26:45–52. https://doi.org/10.1111/j.0141-9838.2004.00682.x
15. Godot V, Harraga S, Deschaseaux M, Bresson-Hadni S, Gottstein B, Emilie D, Vuitton DA. 1997. Increased basal production of interleukin-10 by peripheral blood mononuclear cells in human alveolar echinococcosis. Eur Cytokine Netw 8:401–408.
16. Mondragón-de-la-Peña C, Ramos-Solís S, Barbosa-Cisneros O, Rodríguez-Padilla C, Tavizón-García P, Herrera-Esparza R. 2002. *Echinococcus granulosus* down regulates the hepatic expression of inflammatory cytokines IL-6 and TNFα in BALB/c mice. Parasite 9:351–356. https://doi.org/10.1051/parasite/2002094351
17. Tuxun T, Wang JH, Lin RY, Shan JY, Tai QW, Li T, Zhang JH, Zhao JM, Wen H. 2012. Th17/Treg imbalance in patients with liver cystic echinococcosis. Parasite Immunol 34:520–527. https://doi.org/10.1111/j.1365-3024.2012.01383.x
18. Vismarra A, Mangia C, Passeri B, Brundu D, Masala G, Ledda S, Mariconti M, Brindani F, Kramer L, Bacci C. 2015. Immuno-histochemical study of ovine cystic echinococcosis (*Echinococcus granulosus*) shows predominant T cell infiltration in established cysts. Vet Parasitol 209:285–288. https://doi.org/10.1016/j.vetpar.2015.02.027
19. Nutman TB. 2015. Looking beyond the induction of Th2 responses to explain immunomodulation by helminths. Parasite Immunol 37:304–313. https://doi.org/10.1111/pim.12194
20. Wang H, Zhang C-S, Fang B-B, Li Z-D, Li L, Bi X-J, Li W-D, Zhang N, Lin R-Y, Wen H. 2019. Thioredoxin peroxidase secreted by *Echinococcus granulosus* (sensu stricto) promotes the alternative activation of macrophages via PI3K/AKT/mTOR pathway. Parasit Vectors 12:542. https://doi.org/10.1186/s13071-019-3786-z
21. Cao S, Gong W, Zhang X, Xu M, Wang Y, Xu Y, Cao J, Shen Y, Chen J. 2020. Arginase promotes immune evasion of *Echinococcus granulosus* in mice. Parasites Vectors 13:1–12. https://doi.org/10.1186/s13071-020-3919-4
22. Mourglia-Ettlin G, Merlino A, Capurro R, Dematteis S. 2016. Susceptibility and resistance to *Echinococcus granulosus* infection: associations between mouse strains and early peritoneal immune responses. Immunobiology 221:418–426. https://doi.org/10.1016/j.imbio.2015.11.012
23. Cucher M, Prada L, Mourglia-Ettlin G, Dematteis S, Camicia F, Asurmendi S, Rosenzvit M. 2011. Identification of *Echinococcus granulosus* microRNAs and their expression in different life cycle stages and parasite genotypes. Int J Parasitol 41:439–448. https://doi.org/10.1016/j.ijpara.2010.11.010
24. Seoane PI, Rückerl D, Casaravilla C, Barrios AA, Pittini Á, MacDonald AS, Allen JE, Díaz A. 2016. Particles from the *Echinococcus granulosus* laminated layer inhibit IL-4 and growth factor-driven Akt phosphorylation and proliferative responses in macrophages. Sci Rep 6:39204. https://doi.org/10.1038/srep39204
25. Corraliza IM, Campo ML, Soler G, Modolell M. 1994. Determination of arginase activity in macrophages: a micromethod. J Immunol Methods 174:231–235. https://doi.org/10.1016/0022-1759(94)90027-2
26. Livak KJ, Schmittgen TD. 2001. Analysis of relative gene expression data using real-time quantitative PCR and the 2-ΔΔCT method. Methods 25:402–408. https://doi.org/10.1006/meth.2001.1262
27. Bain CC, Jenkins SJ. 2018. Isolation and identification of murine serous cavity macrophages. Methods Mol Biol 1784:51–67. https://doi.org/10.1007/978-1-4939-7837-3_5
28. Finlay CM, Parkinson JE, Zhang L, Chan BHK, Ajendra J, Chenery A, Morrison A, Kaymak I, Houlder EL, Murtuza Baker S, Dickie BR, Boon L, Konkel JE, Hepworth MR, MacDonald AS, Randolph GJ, Rückerl D, Allen JE. 2023. T helper 2 cells control monocyte to tissue-resident macrophage differentiation during nematode infection of the pleural cavity. Immunity 56:1064–1081. https://doi.org/10.1016/j.immuni.2023.02.016
29. Loke P, Nair MG, Parkinson J, Guiliano D, Blaxter M, Allen JE. 2002. IL-4 dependent alternatively-activated macrophages have a distinctive *in vivo* gene expression phenotype. BMC Immunol 3:7. https://doi.org/10.1186/1471-2172-3-7
30. Coakley G, Harris NL. 2020. Interactions between macrophages and helminths. Parasite Immunol 42:1–13. https://doi.org/10.1111/pim.12717
31. Dyck L, Mills KHG. 2017. Immune checkpoints and their inhibition in cancer and infectious diseases. Eur J Immunol 47:765–779. https://doi.org/10.1002/eji.201646875
32. Smith P, Walsh CM, Mangan NE, Fallon RE, Sayers JR, McKenzie ANJ, Fallon PG. 2004. Schistosoma mansoni worms induce anergy of T cells via selective up-regulation of programmed death ligand 1 on macrophages. J Immunol 173:1240–1248. https://doi.org/10.4049/jimmunol.173.2.1240
33. Terrazas LI, Montero D, Terrazas CA, Reyes JL, Rodríguez-Sosa M. 2005. Role of the programmed death-1 pathway in the suppressive activity of alternatively activated macrophages in experimental cysticercosis. Int J Parasitol 35:1349–1358. https://doi.org/10.1016/j.ijpara.2005.06.003
34. Huber S, Hoffmann R, Muskens F, Voehringer D. 2010. Alternatively activated macrophages inhibit T-cell proliferation by Stat6-dependent expression of PD-L2. Blood 116:3311–3320. https://doi.org/10.1182/blood-2010-02-271981
35. van der Werf N, Redpath SA, Azuma M, Yagita H, Taylor MD. 2013. Th2 cell-intrinsic hypo-responsiveness determines susceptibility to helminth infection. PLoS Pathog 9:e1003215. https://doi.org/10.1371/journal.ppat.1003215
36. Stempin CC, Motrán CC, Aoki MP, Falcón CR, Cerbán FM, Cervi L. 2016. PD-L2 negatively regulates Th1-mediated immunopathology during Fasciola hepatica infection. Oncotarget 7:77721–77731. https://doi.org/10.18632/oncotarget.12790
37. Chen X, Oppenheim JJ, Howard OMZ. 2005. BALB/c mice have more CD4+CD25+ T regulatory cells and show greater susceptibility to suppression of their CD4+CD25- responder T cells than C57BL/6 mice. J Leukoc Biol 78:114–121. https://doi.org/10.1189/jlb.0604341
38. Thomas JA, Kothare SN. 1975. Tissue response in hydatidosis. Indian J Med Res 63:1761–1766.
39. Rückerl D, Allen JE. 2014. Macrophage proliferation, provenance, and plasticity in macroparasite infection. Immunol Rev 262:113–133. https://doi.org/10.1111/imr.12221
40. Barrios AA, Mouhape C, Schreiber L, Zhang L, Nell J, Suárez-Martins M, Schlapp G, Meikle MN, Mulet AP, Hsu T-L, Hsieh S-L, Mourglia-Ettlin G, González C, Crispo M, Barth TFE, Casaravilla C, Jenkins SJ, Díaz Á. 2023. Mucins shed from the laminated layer in cystic echinococcosis are captured by Kupffer cells via the lectin receptor Clec4F Infect Immun 91:e0029923. https://doi.org/10.1128/iai.00299-23
41. Locati M, Curtale G, Mantovani A. 2020. Diversity, mechanisms, and significance of macrophage plasticity. Annu Rev Pathol 15:123–147. https://doi.org/10.1146/annurev-pathmechdis-012418-012718
42. Dong D, Chen C, Hou J, Yang K, Fang H, Jiang H, Guo F, Wu X, Chen X. 2019. KLF4 upregulation is involved in alternative macrophage activation during secondary *Echinococcus granulosus* infection. Parasite Immunol 41:e12666. https://doi.org/10.1111/pim.12666
43. La X, Zhang F, Li Y, Li J, Guo Y, Zhao H, Pang N, Ma X, Wen H, Fan H, Ding J. 2015. Upregulation of PD-1 on $CD4^+CD25^+$T cells is associated with immunosuppression in liver of mice infected with Echinococcus multilocularis. Int Immunopharmacol 26:357–366. https://doi.org/10.1016/j.intimp.2015.04.013

44. Terrazas C, de Dios Ruiz-Rosado J, Amici SA, Jablonski KA, Martinez-Saucedo D, Webb LM, Cortado H, Robledo-Avila F, Oghumu S, Satoskar AR, Rodriguez-Sosa M, Terrazas LI, Guerau-de-Arellano M, Partida-Sánchez S. 2017. Helminth-induced Ly6Chi monocyte-derived alternatively activated macrophages suppress experimental autoimmune encephalomyelitis. Sci Rep 7:40814. https://doi.org/10.1038/srep40814
45. Campbell SM, Knipper JA, Ruckerl D, Finlay CM, Logan N, Minutti CM, Mack M, Jenkins SJ, Taylor MD, Allen JE. 2018. Myeloid cell recruitment versus local proliferation differentiates susceptibility from resistance to filarial infection. Elife 7:1–17. https://doi.org/10.7554/eLife.30947
46. Rodriguez PC, Zea AH, DeSalvo J, Culotta KS, Zabaleta J, Quiceno DG, Ochoa JB, Ochoa AC. 2003. L-arginine consumption by macrophages modulates the expression of CD3ζ chain in T lymphocytes. J Immunol 171:1232–1239. https://doi.org/10.4049/jimmunol.171.3.1232
47. Jubel JM, Barbati ZR, Burger C, Wirtz DC, Schildberg FA. 2020. The role of PD-1 in acute and chronic infection. Front Immunol 11:487. https://doi.org/10.3389/fimmu.2020.00487
48. Miggelbrink AM, Jackson JD, Lorrey SJ, Srinivasan ES, Waibl-Polania J, Wilkinson DS, Fecci PE. 2021. CD4 T-cell exhaustion: does it exist and what are its roles in cancer? Clin Cancer Res 27:5742–5752. https://doi.org/10.1158/1078-0432.CCR-21-0206
49. Zhang C, Shao Y, Yang S, Bi X, Li L, Wang H, Yang N, Li Z, Sun C, Li L, Lü G, Aji T, Vuitton DA, Lin R, Wen H. 2017. T-cell tolerance and exhaustion in the clearance of Echinococcus multilocularis: role of inoculum size in a quantitative hepatic experimental model. Sci Rep 7:11153. https://doi.org/10.1038/s41598-017-11703-1
50. Pan W, Zhou H-J, Shen Y-J, Wang Y, Xu Y-X, Hu Y, Jiang Y-Y, Yuan Z-Y, Ugwu CE, Cao J-P. 2013. Surveillance on the status of immune cells after *Echinnococcus granulosus* protoscoleces infection in BALB/c mice. PLoS One 8:e59746. https://doi.org/10.1371/journal.pone.0059746
51. Francisco LM, Salinas VH, Brown KE, Vanguri VK, Freeman GJ, Kuchroo VK, Sharpe AH. 2009. PD-L1 regulates the development, maintenance, and function of induced regulatory T cells. J Exp Med 206:3015–3029. https://doi.org/10.1084/jem.20090847
52. Maizels RM. 2021. The multi-faceted roles of TGF-β in regulation of immunity to infection. Adv Immunol 150:1–42. https://doi.org/10.1016/bs.ai.2021.05.001
53. Wang J, Zhang C, Wei X, Blagosklonov O, Lv G, Lu X, Mantion G, Vuitton DA, Wen H, Lin R, De Re V. 2013. TGF-β and TGF-β/smad signaling in the interactions between *Echinococcus* multilocularis and its hosts. PLoS One 8:e55379. https://doi.org/10.1371/journal.pone.0055379
54. Pang N, Zhang F, Ma X, Zhu Y, Zhao H, Xin Y, Wang S, Chen Z, Wen H, Ding J. 2014. TGF-β/smad signaling pathway regulates Th17/Treg balance during *Echinococcus* multilocularis infection. Int Immunopharmacol 20:248–257. https://doi.org/10.1016/j.intimp.2014.02.038
55. Mejri N, Müller J, Gottstein B. 2011. Intraperitoneal murine *Echinococcus* multilocularis infection induces differentiation of TGF-β-expressing DCs that remain immature. Parasite Immunol 33:471–482. https://doi.org/10.1111/j.1365-3024.2011.01303.x
56. Mejri N, Müller N, Hemphill A, Gottstein B. 2011. Intraperitoneal *Echinococcus* multilocularis infection in mice modulates peritoneal CD4+ and CD8+ regulatory T cell development. Parasitol Int 60:45–53. https://doi.org/10.1016/j.parint.2010.10.002
57. Liu Y, Abudounnasier G, Zhang T, Liu X, Wang Q, Yan Y, Ding J, Wen H, Yimiti D, Ma X. 2016. Increased expression of TGF-β1 in correlation with liver fibrosis during *Echinococcus granulosus* infection in mice. Korean J Parasitol 54:519–525. https://doi.org/10.3347/kjp.2016.54.4.519
58. Rogan MT. 1998. T-cell activity associated with secondary infections and implanted cysts of *Echinococcus granulosus* in BALB/c mice. Parasite Immunol 20:527–533. https://doi.org/10.1046/j.1365-3024.1998.00180.x
59. Palomo J, Dietrich D, Martin P, Palmer G, Gabay C. 2015. The interleukin (IL)-1 cytokine family--balance between agonists and antagonists in inflammatory diseases. Cytokine 76:25–37. https://doi.org/10.1016/j.cyto.2015.06.017
60. Casaravilla C, Pittini Á, Rückerl D, Allen JE, Díaz Á. 2020. Activation of the NLRP3 inflammasome by particles from the *Echinococcus granulosus* laminated layer. Infect Immun 88:e00190-20. https://doi.org/10.1128/IAI.00190-20
61. Filbey KJ, Varyani F, Harcus Y, Hewitson JP, Smyth DJ, McSorley HJ, Ivens A, Nylén S, Rottenberg M, Löser S, Maizels RM. 2019. Macrophage migration inhibitory factor (MIF) is essential for type 2 effector cell immunity to an intestinal helminth parasite. Front Immunol 10:2375. https://doi.org/10.3389/fimmu.2019.02375
62. Prieto-Lafuente L, Gregory WF, Allen JE, Maizels RM. 2009. MIF homologues from a filarial nematode parasite synergize with IL-4 to induce alternative activation of host macrophages. J Leukoc Biol 85:844–854. https://doi.org/10.1189/jlb.0808459
63. Donnelly S, Stack CM, O'Neill SM, Sayed AA, Williams DL, Dalton JP. 2008. Helminth 2 - Cys peroxiredoxin drives Th2 responses through a mechanism involving alternatively activated macrophages. FASEB J 22:4022–4032. https://doi.org/10.1096/fj.08-106278
64. Mitre E, Klion AD. 2021. Eosinophils and Helminth infection: protective or pathogenic? Semin Immunopathol 43:363–381. https://doi.org/10.1007/s00281-021-00870-z